

RSC Advances



This is an *Accepted Manuscript*, which has been through the Royal Society of Chemistry peer review process and has been accepted for publication.

Accepted Manuscripts are published online shortly after acceptance, before technical editing, formatting and proof reading. Using this free service, authors can make their results available to the community, in citable form, before we publish the edited article. This *Accepted Manuscript* will be replaced by the edited, formatted and paginated article as soon as this is available.

You can find more information about *Accepted Manuscripts* in the [Information for Authors](#).

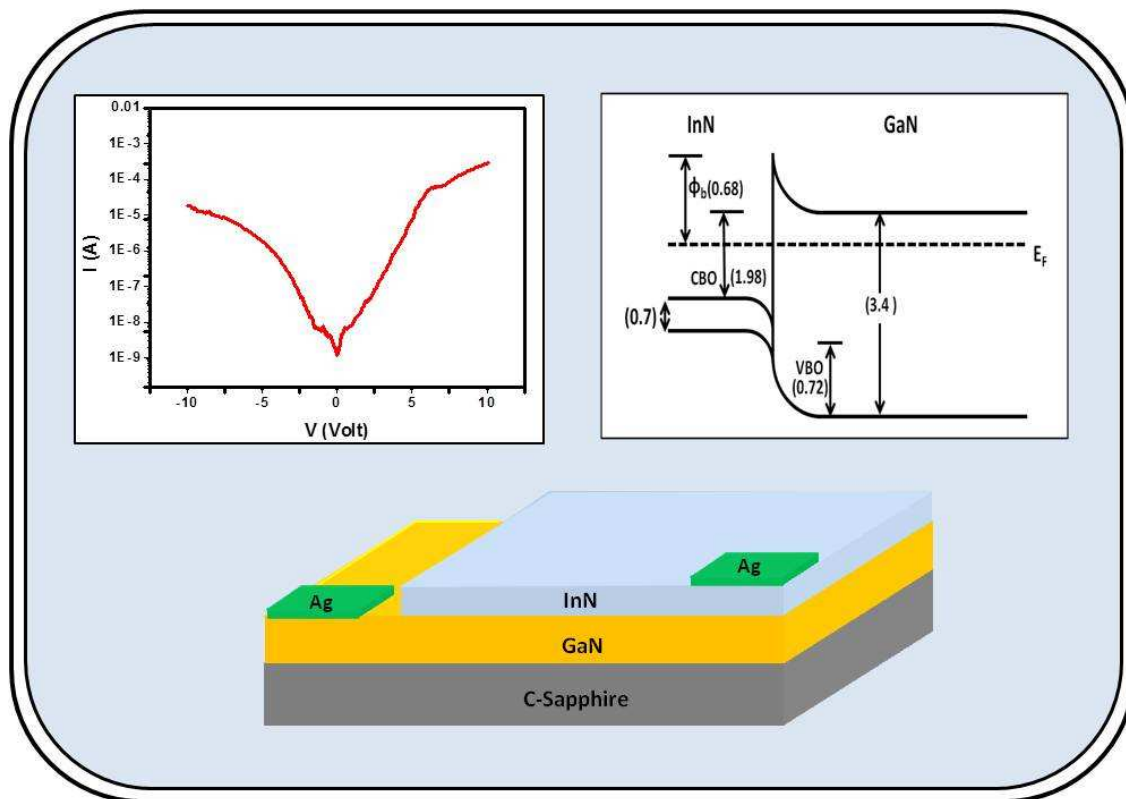
Please note that technical editing may introduce minor changes to the text and/or graphics, which may alter content. The journal's standard [Terms & Conditions](#) and the [Ethical guidelines](#) still apply. In no event shall the Royal Society of Chemistry be held responsible for any errors or omissions in this *Accepted Manuscript* or any consequences arising from the use of any information it contains.

Band alignment and Schottky behaviour of InN/GaN heterostructure grown by nitrogen ions

Shibin Krishna T.C^a. and Govind Gupta^{a*}

Physics of Energy Harvesting, National Physical Laboratory (CSIR-NPL), Dr. K.S. Krishnan Road, New Delhi-110012 (India).

Graphical Abstract



InN/GaN heterostructure based Schottky diodes are fabricated by low energetic Nitrogen ions at 300°C.

RSC Advances

Cite this: *RSC Advances*, xxxx, x ,xxxx-xxxx

www.rsc.org/advances

PAPER

Band alignment and Schottky behaviour of InN/GaN heterostructure grown by low-temperature low-energy nitrogen ion bombardment

Shibin Krishna T.C^a. and Govind Gupta^{a*}

Received :

DOI:

InN/GaN heterostructure based Schottky diodes are fabricated by reactive Low Energy Nitrogen Ion (LENI) bombardment at low substrate temperature (300°C). The valence band offset (VBO) of nitrogen ion induced In-polar InN/GaN hetero-interface has been analyzed by X-ray photoelectron spectroscopy and it is determined to be 0.72±0.28 eV, a type-I straddled band alignment is formed at the InN/GaN interface. Fermi level pinning is observed to be 1.3±0.1 eV above the conduction band minimum resulting a strong downward band bending. Valence band maxima of InN/GaN show that the surface electron accumulation occurs due to the presence of In adlayer on the film. Atomic Force Microscopy analysis divulged the formation of step like InN structure on GaN surface. I-V characteristic showed that the junction between InN and GaN exhibit a Schottky type behaviour. The room temperature barrier height and the ideality factor of the InN/GaN Schottky diodes are calculated by using thermionic emission (TE) model and found to be 0.72 eV and 20.8 respectively.

Introduction

The studies of III-nitride hetero-interface have shown immense importance due to their potential applications in solid state lighting and photovoltaic devices.¹⁻⁵ The recent advancement in the growth technologies has significantly improved the crystal quality of InN,⁶⁻¹⁰ however the lack of lattice matched substrates, low dissociation temperature and the high equilibrium vapour pressure of Nitrogen¹¹ are still posing challenges to the growth of InN. These constraints lead to the formation of dislocations and strain in the grown epitaxial film resulting in the degradation of the device performance.¹² A number of buffer techniques and different substrate materials have been employed in order to conquer the difficulty of large lattice mismatch between substrate and InN.¹³⁻¹⁵ In addition to the many physical properties of InN such as low band gap (0.64 eV),¹⁶ high mobility (500-3000 cm²/V-s)¹⁷ etc, interface studies of InN and their alloys (InGaN, InAlN) with other semiconductor has raised more interest in device application. Interestingly, the InN/GaN hetero-interface displays characteristic feature of a Schottky diode¹⁸ which is a direct measure of rectifying behaviour at the semiconductor interface. Although GaN based Schottky diodes with different metal contacts have been studied by several groups,¹⁹⁻²¹ but there are few reports on InN/GaN based Schottky diodes.^{18,22,23} Detailed knowledge of rectifying behaviour between InN and GaN interface are crucial for obtaining the fundamental understanding of the heterostructure. Further, the large difference in the band gaps of InN¹⁶ and GaN²⁴ implies that the valence & conduction band offset plays a significant role in designing of the band diagram and thus the accurate determination of the band offset is essential.¹³ Number of studies has been performed to investigate the valence band offset (VBO) of InN with other III-N semiconductors,^{13,25} however studies of InN/GaN based Schottky diode are still not premeditated. Further, the unusual phenomena of surface electron accumulation (SEA), the electrons move freely parallel to the interface or two dimensional electron gas (2DEG), at as-grown InN surface²⁶⁻²⁸ is proposed to be one of the key issues to

^aPhysics of Energy Harvesting, National Physical Laboratory (CSIR-NPL), Dr. K.S. Krishnan Road, New Delhi-110012 (India).

enable further progress in the InN based technology which can be determined by VBO. The consequence of SEA-phenomena causes Fermi level pinning which still posing challenges²⁶ for as-grown InN/GaN heterostructures. This pinning has also been observed experimentally by irradiation of defects induced energetic particle on group III-nitrides (InN, GaN) and on In rich alloys (InGaN).²⁹

The quantized electron accumulation can also significantly alter band gap property, which guide a new route to spatially inhomogeneous band gap engineering.³⁰ However, the physical origin of this phenomenon is not yet unambiguously clear, and has been attributed not only for both polar and non-polar surfaces³¹ but also to the presence of donor like surface states.³² Thus, the detailed knowledge of SEA is required for obtaining the basic understanding of the electronic properties of InN and for designing of InN/GaN heterostructure based optoelectronic & photovoltaic devices.

In this work, reactive low energy sputtering (Nitrogen ion) technique has been employed for InN formation on GaN template. We have experimentally demonstrated the effect of In adlayer on VBO of low temperature and low energy nitrogen ion (LENI) induced InN/GaN hetero-interface by X-ray photoelectron spectroscopy (XPS) which provides a better understanding of SEA phenomena. The calculation of InN/GaN valence band offset can provide an exact idea of band structure of hetero-interface. The Atomic force microscopy (AFM) examination revealed the morphological properties of grown InN surface and the effects of rectifying behaviour of InN/GaN hetero-interface have been investigated by I-V characteristics where the room temperature barrier height and the ideality factor of the Schottky diodes are calculated to be 0.72 eV and 20.8 respectively.

Experimental Techniques

In and InN were grown on a GaN template (MOCVD grown-3.5 μm) on c-plane sapphire substrate³³ in UHV system equipped with X-ray photoelectron spectroscopy at base pressure 5.0×10^{-11} torr. The GaN samples were cleaned (ambient) by modified Shiraki process³⁴ and then prepared in-situ by annealing at 600°C (4 hours) and rapid flashing at 900°C (5 sec) followed by slow cooling to room temperature (RT) which was further cleaned by 1keV-LENI at 600°C (3 hours). Homemade tantalum Knudsen cell was used to evaporate Indium metal (CERAC, 99.999%) by circulating the current to control the evaporated material flux (10 nm/min). Indium was deposited for 1 min on GaN followed by nitridation at low temperature (300°C) to form InN/GaN heterostructures using 300 eV-LENI. We have grown number of samples with same nitridation parameter (300 eV and 300°C) and different nitridation time (60 min, 120 min, and 180 min) in order to study the In to InN conversion by LENI. This technique is relatively inexpensive and simpler growth approach which offers the possibility of growth at lower temperatures. The ion beam used in this technique have benefits like selecting the ion beam energy, simplicity of focusing and have ability to alter the chemical nature of the materials with unique properties. The details of this technique is explained elsewhere.^{35,36} The XPS measurements of GaN, InN/GaN samples were performed with Omicron-Multiprobe Surface Analysis System using $\text{Mg}_{K\alpha}$ X-ray source (1253.6 eV). The calibration of electron binding energy was performed with the Fermi edge of a clean Silver reference sample. The core level (CL) spectra of Ga 3d & In 3d have been fitted by using Shirley background and Gaussian line shape.¹⁰ The position of valence band maximum was determined by extrapolating a linear fit to the leading edge of the valence band maximum (VBM). The surface morphology of the GaN substrate and InN/GaN surface was analysed by NT-MDT Solver Pro-Atomic Force Microscopy (AFM). I-V measurements were performed by depositing two Ag metal contacts on InN and GaN layers and measurements were carried out by using computer interfaced Keithley-2400 source meter system at room temperature. It is important to mention that the contact resistance of Ag/GaN and Ag/InN will not affect the measured results due to the high material resistance of GaN and InN. The thickness of the grown InN layer was estimated from the Secondary Ions Mass Spectroscopy (SIMS) depth profile data where Cs^+ ions with 1 keV energy were used for sputtering the sample.

Results and Discussion

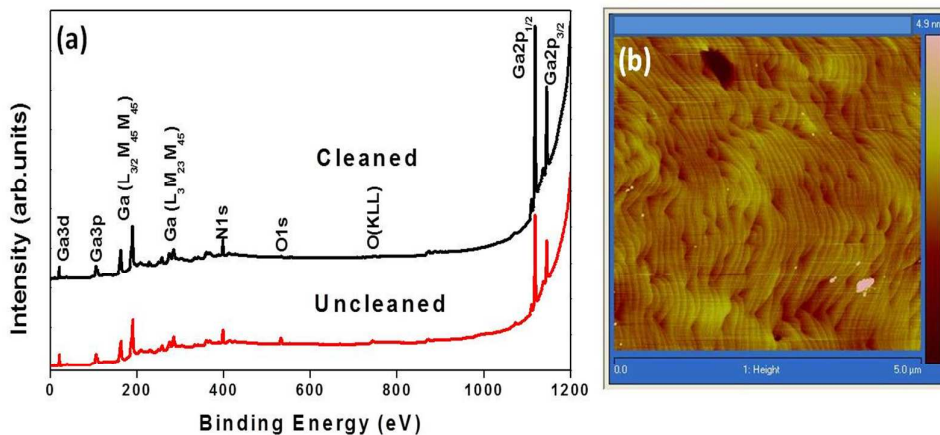


Figure 1. (a) XPS survey scan of GaN/C-plane sapphire substrate i) Uncleaned ii) Cleaned (b) AFM image of clean GaN template.

Fig 1a shows the XPS survey scan of pre- and post- cleaned GaN template where the presence of Ga ($2p_{1/2}$, $2p_{3/2}$, $3p$, $3d$) and Nitrogen ($1s$) is observed at binding energies (BEs) of 1157.0 eV, 1118.0 eV, 105.0 eV, 19.5 eV and 399.5 eV respectively along with Ga Auger (LMM) peaks at 162.0 eV, 189.0 eV, 275.0 eV and 284.0 eV. Oxygen $1s$ (531.0 eV) and O Auger-KLL (743.0 eV) peaks were also detected (surface contamination) in the uncleaned sample which were almost disappeared after the cleaning process. The morphology of the MOCVD grown clean GaN surface was examined by AFM (fig 1b) which shows a smooth surface, consists of array of terraces (width ~ 100 nm) with rms roughness of 0.398 nm. The template contains large number of pits (originated due to misfit dislocations between substrate & GaN film) where many of the terraces terminate at the edges of pit. These pits terminating on the step leads to the surface termination of a mixed character threading dislocation having a screw component with Burgers vector equal to the c-axis lattice parameter of GaN $\sim (5.2 \text{ \AA})$. A detailed study of dislocation mediated structure of GaN surface is reported by Heying et.al.³⁷ From fig 1b, the total density of pits on GaN surface is calculated to be $\sim 6.4 \times 10^8/\text{cm}^2$. These results are consistent with the AFM results of Ga-polar GaN sample reported by Kim et.al.³⁸

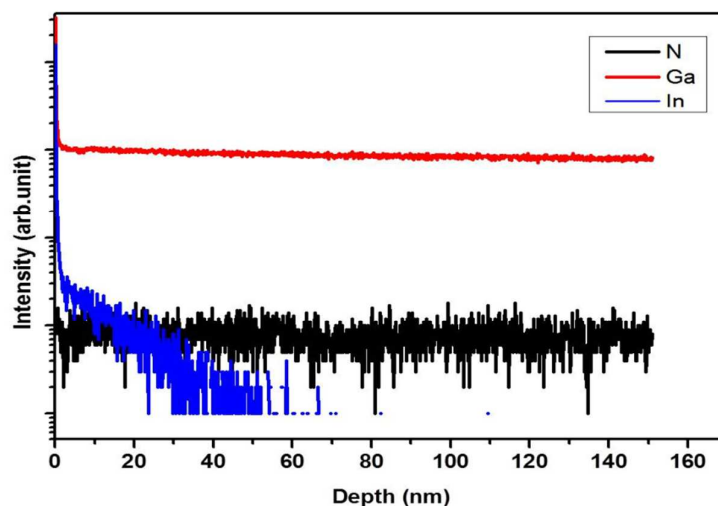


Figure 2. Depth profile of InN/GaN heterostructure

InN/GaN heterostructures are grown at 300 °C substrate temperature using 300 eV nitrogen ions for 180 minutes. To measure the thickness of the InN film on GaN, the depth profile of InN/GaN hetero-structure was carried out using TOF-SIMS as shown in Fig. 2. SIMS spectra revealed the presence of Ga, In and N and signals where the N signal can be seen steadily throughout the profile due to the presence of N in all the layers (both InN and GaN). The SIMS analysis divulge that the thickness of InN is ~10-12 nm followed by diffusion of In atoms in GaN films for ~ 10-15 nm. The mass spectrum of Indium (mass number 115 amu) during SIMS measurement has also been included as a figure S1 which shows the presence of Indium in the grown film. The structural characterization of InN/GaN hetero-interface was carried out by Grazing Incident X-ray diffraction (GI-XRD) to confirm the formation of InN. A small peak at 31.5° was observed which correspond to wurtzite InN (0002) plane (GI-XRD plot is given in supporting document as figure S2).

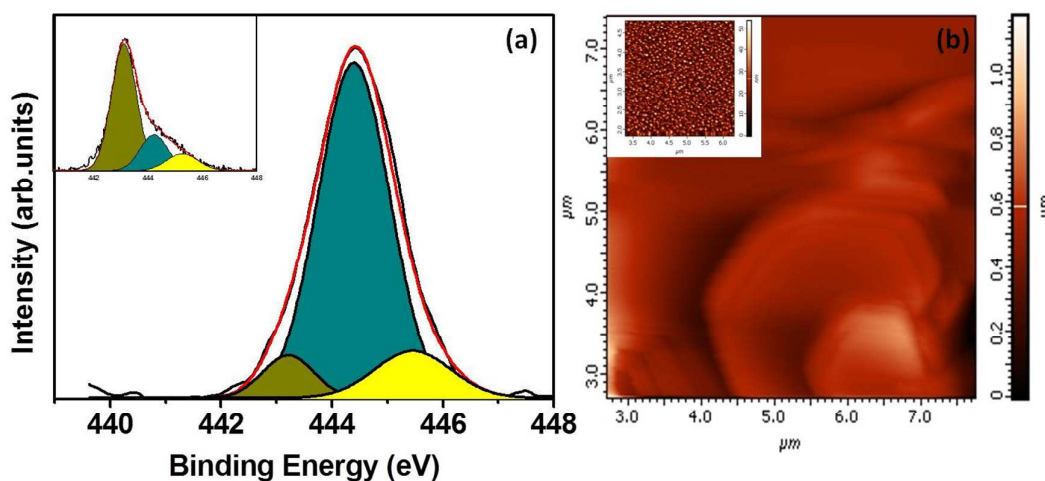


Figure 3. (a) Deconvoluted XPS Core level spectra of In ($3d_{5/2}$) for high coverage InN film, inset shows for low coverage InN film. (b) AFM image of InN film on GaN showing step like structure, inset shows surface morphology of low coverage InN film.

Photoemission analysis was carried out to understand the surface chemistry, composition, band alignment & valence band offset of the grown InN/GaN heterostructure. The CL spectra of In $3d_{5/2}$ of InN/GaN heterostructure is shown in fig 3a. In $3d_{5/2}$ spectra is deconvoluted into three components: the component at BE 443.1eV displays the presence of In-In bond (metallic indium adlayer), peak at BE 444.2eV attributed to In-N bonding while the higher BE peak (445.3eV) can be attributed to inelastic losses of the conduction electrons in the charge accumulation layer.³⁹ The deconvoluted core level peak of InN film shows the dominant coverage of InN (81%) along with small amount of metallic In-In (7%). The presence of metallic bond signifies either the lack of reactive nitrogen or the desorption of nitrogen from the surface which is similar to the occurrence of Ga adlayers at Ga- and N-polar GaN surfaces.^{40,41} Further the metallic adlayer (In-In bond) results from the large size difference between the cation (In) and anion (N) making such reconstruction energetically favourable which indicates one of the possible origins of surface electron accumulation,⁴² resulting the downward band bending in the system. For the comparative understanding of metal adlayer on the InN/GaN heterostructure interface, we have grown a number of InN/GaN heterostructures under the similar nitridation conditions (300 eV at 300°C) at different nitridation time (60 min, 120 min). Inset of fig 3a, shows the XPS core level spectra of In $3d_{5/2}$ of 60 min nitridated sample in which the component corresponding to metallic adlayer (61%) dominates and a moderate conversion of In to InN (23%) has been observed.

The surface morphology of the InN (180 min LENI 300 eV, 300°C) sample is shown in fig. 3b. The AFM image shows the step like structure with large terraces (>1 μm width) separated by ~2-3 Å step height. The 180 min exposure of LENI leads to the removal of some of the In atoms from the surface followed by the formation of thin InN layer on the GaN surface. The surface features consisted of spiral growth with hexagonal boundaries having surface roughness of 0.3 nm. Similar step like morphology of InN/GaN with spiral growth at substrate temperatures higher than 540°C by MBE is reported by Wang et.al⁴³. This suggests that with reactive ion technique, good quality InN can be grown at sufficiently low temperature (300°C). Inset fig 3b displays the surface morphology of low InN surface grown at 300°C using 300 eV LENI for 60min which illustrates the large number of granular InN nanostructures (surface roughness 6.28 nm) on the GaN surface. Dimakis et.al⁴⁴ reported similar surface morphology of InN by MBE at 350°C substrate temperature. The formation of InN granular structure at low

temperature is explained through LENI induced sputtering which leads to the island formation by the stabilization of low energy nitrogen ions on the surface. Fareed et.al.⁴⁵ have suggested that the strain (lattice mismatch, growth parameters etc) in the grown InN surface can be relaxed by two mechanisms; either by island formation and/or by defect generation.

The VB spectra of GaN substrate and the grown InN (300eV, 180 min) thin film have been shown in fig 4a. The energy structure of InN/GaN heterostructure is identified by VB spectra where the coincidence of the leading edge of the VB gives the VBM to Fermi level (E_F) separation.⁴⁶ The separation between VBM to E_F for GaN sample is found to be 1.85 ± 0.1 eV (fig 3a (i)), indicates a Gallium terminating GaN surface (Ga-face GaN).⁴⁷ The surface E_F is 1.55 ± 0.1 eV below (band gap of GaN ~ 3.4 eV²⁴) the bottom conduction band (CB) edge, indicating nearly intrinsic property. The emission close to E_F (shown by an arrow in VB spectra in fig 4a (i)) is associated with metallic density of states due to the presence of metallic Gallium (Ga-Ga) on the surface¹¹ which contributes for surface electron accumulation. The peaks at 11 eV and 9 eV in the VB spectra correspond to the presence of N 2s bonding and plasmonic excitation respectively.^{48,49} The VB spectra of InN has shown in fig 4a (ii) where the VB maximum (VBM) to E_F separation is observed to be 2.0 ± 0.1 eV. Considering the band gap of InN ~ 0.7 eV,¹⁶ the Fermi level is pinned to 1.30 ± 0.1 eV above the conduction band minima (CBM). Anomalous downward band bending observed in InN has been attributed to the large difference in electro-negativity between In and N atoms, causing difficulty in the formation of high resistive InN films.⁵⁰ The VB spectra can also divulge the polarity of InN material by comparing the intensity ratio of 3.8eV and 6.5eV VB peaks^{51,52} (indicated in the VB spectra in fig 4a (ii)). Here, InN VB spectra confirmed In-face polarity of InN/GaN heterojunction.

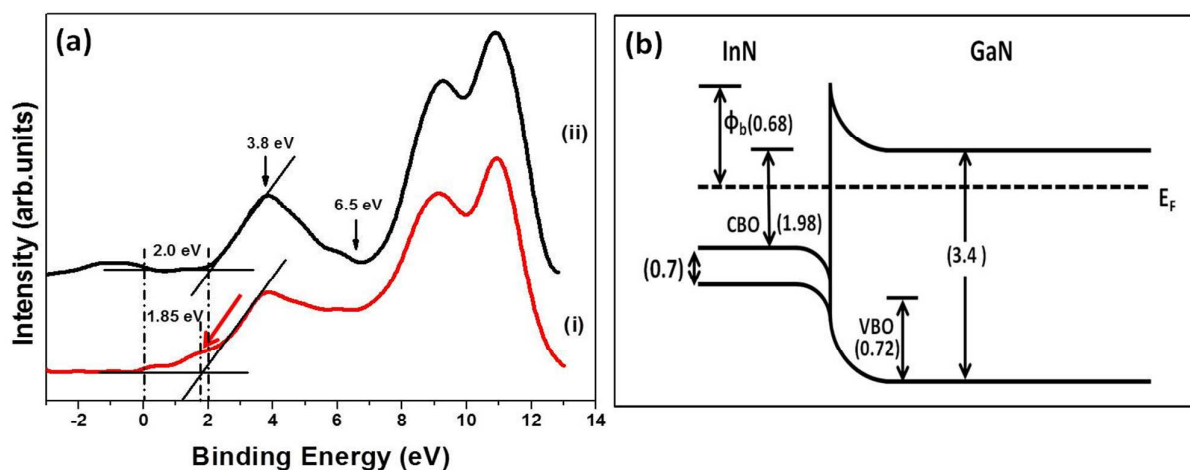


Figure 4. (a) (i) Valence band spectra of GaN substrate and (ii) InN/GaN heterojunction, (b) Schematic of Energy band diagram for the InN/GaN heterojunction. A type-I heterojunction is formed in the straddled arrangement.

Further, an exact band structure of InN/GaN hetero-interface can be determined by estimating the VBO (ΔE_V) value.⁵³ The VBO values can be calculated by the following equation,

$$\Delta E_V = \Delta E_{CL} - (E_{3d5/2} - E_{VBM})^{\text{InN}} + (E_{3d} - E_{VBM})^{\text{GaN}} \quad (1)$$

where, $\Delta E_{CL} = (E_{3d5/2})^{\text{InN}} - (E_{3d})^{\text{GaN}}$

ΔE_{CL} is the core level energy separation between measured In_{3d} and Ga_{3d} spectra of the InN/GaN heterostructures. The two terms, $(E_{CL} - E_{VBM})^{\text{Material}}$, are separation between a core level and VBM of the thick InN and GaN samples. Schematic of the energy band diagram for the InN/GaN heterojunction is shown in fig 4b. The experimental error was calculated by considering the fitting errors and the discrepancy between repeated measurements (± 130 meV) for E_{CL} and for the two $(E_{CL} - E_{VBM})$ components (± 50 meV) in Eq. 1. Therefore the total error for ΔE_V is calculated to be ± 230 meV. Fitting by numerical calculations introduce an additional error of ± 50 meV resulting in a total error of ± 280 meV. Hence, the calculated VBO is 0.72 ± 0.28 eV which is slightly higher than the theoretical (0.45 eV) value suggested by Van de Walle et al.⁵⁴ and lower than the experimental value of 1.05 ± 0.25 eV by Martin et al.¹³. To improve the accuracy of the InN/GaN VBO⁵⁵, the binding energies of other In ($3s$, $3p_{3/2}$) and Ga ($3p_{3/2}$, $2p_{3/2}$) core level peaks were also determined as listed in Table 1. InN/GaN VBO

derived from different set of XPS core level peaks are given in Table 2. The average InN/GaN VBO calculated using different core level is found to be 0.76 ± 0.28 eV.

Due to the presence of In adlayer on the hetero-interface, the Fermi level pinning (1.3 ± 0.1 eV) is observed in the conduction band of InN/GaN heterostructure. The band line up is determined with a conduction band offset (CBO) or ΔE_c as 1.98 ± 0.28 eV based on the above ΔE_v value, shown in fig 3b. The observed value of ΔE_c is found to be lower than the theoretically predicted value (2.3 ± 0.28 eV)⁵⁴. Hence, a strong band bending is observed on the InN side which is the consequence of the presence of SEA at InN/GaN interface. Due to the large barrier at the InN/GaN heterojunction, the excess electron density variation should be similar to that of 2DEG⁵⁶ (confirmed by VB spectra). The presence of a 2DEG near the surface of a semiconductor can significantly alter the size of its band gap through many-body effects caused by its high electron density, resulting in a surface band gap which differs from its value in the bulk of the material.³⁰ According to these results, a type-I band alignment is formed at the InN/GaN heterojunction in the straddled arrangement as shown in Fig 4b. However, a flat band was also observed for N-polar stoichiometric InN surfaces after removal of the In-adlayer⁵⁷ and for non-polar (a- and m-plane) in-situ grown, stoichiometric InN.⁵⁸

TABLE 1. Binding energy (eV) of the XPS core level peak in the InN/GaN, InN and GaN.

	InN/GaN	InN	GaN
In 3d_{5/2}	444.38	444.62	
In 3p_{3/2}	665.44	665.72	
In 3s	826.28	826.53	
Ga 3d	19.58		19.35
Ga 3p_{3/2}	105.34		105.05
Ga 2p_{3/2}	1117.62		1117.38

TABLE 2. InN/GaN VBO calculated using different set of XPS core level.

	In 3d _{5/2}	In 3p _{3/2}	In 3s
Ga 3d	0.72	0.76	0.73
Ga 3p_{3/2}	0.78	0.82	0.79
Ga 2p_{3/2}	0.73	0.77	0.74

The room temperature Current-Voltage (I-V) measurement for InN/GaN heterojunction is shown in Fig 5. For high quality InN grown film (fig 5a), a Schottky diode⁵⁹ behaviour is observed; i.e. the junction between InN and GaN exhibited strong rectifying behaviour (the current at the forward bias of 10.0 V is 1.0mA, at a reverse bias of -10 V is -61μA). For low coverage InN film (fig 5b), the current (I) is found to be 1.3 mA at a forward bias voltage of 10 V and for reverse bias -10 V it is 0.6 mA. Therefore a linear behaviour was found in the forward and reverse bias, symmetry showing the metallic (ohmic) behaviour. Ohmic behaviour suggests the presence of SEA phenomena at the InN/GaN hetero-interface which cause the pinning of Fermi level above the conduction band minima (CBM).⁶⁰ According to Thermionic Emission (TE) theory, the forward I-V characteristic of a Schottky diode is given by

$$I = I_s \exp \left(\frac{(q(V) - IR_s)}{\eta kT} \right) \quad (2)$$

$$I_s = AA^* T^2 \exp \left(-\frac{\phi_b}{kT} \right) \quad (3)$$

where I_s is the saturation current density, T is the absolute temperature, A is the active device area ($7 \times 3 \text{ mm}^2$), A^* is the Richardson's constant, k is the Boltzmann constant, q is the electron charge, ϕ_b is the Schottky barrier height, and η is the ideality factor. The values of ϕ_b and η for the Schottky diodes were calculated by fitting Eq.(2) in the linear region of the forward I-V curves ignoring the series resistance (R_s). For calculation, the value of A^* was taken as $6 \text{ A cm}^{-2} \text{ K}^{-2}$ for InN⁶¹. The values of Schottky barrier height (SBH) were calculated to be 0.72 eV and 0.51 eV while ideality factor is found to be 20.8 and 44.1 for high and low InN sample respectively. SBH has also been shown in the energy band diagram for the InN/GaN heterojunction (fig 4b) where the SBH value from I-V (0.72 eV) is in good agreement with the energy band diagram value (0.68 ± 0.1 eV). The higher value of barrier height (0.72 eV) and lower value of ideality factor (20.8) of the diode fabricated

from high quality InN film on GaN film point out the good rectifying nature. This high ideality factor value could be due to the high series resistance (R_s) at the higher applied voltage. Fitting of Eq.(2) without neglecting series resistance did not follow the measured I-V characteristics of the diodes. This result illustrates that in the present case, the thermionic emission over the Schottky barrier is suppressed at higher applied voltages by other current transport mechanisms. The linearity behaviour of InN/GaN Schottky diode disappeared at higher applied voltage, this illustrate by the current transport follows power-law ($I \sim V^{1.6}$).⁶² It was found that the rectifying behaviour of the diodes is defined as in terms of I_F/I_R at certain applied voltage. The ratio at 10 V is 16.4 and 2.16 for the respective samples; i.e. the Schottky diodes with high InN have good rectifying capability.

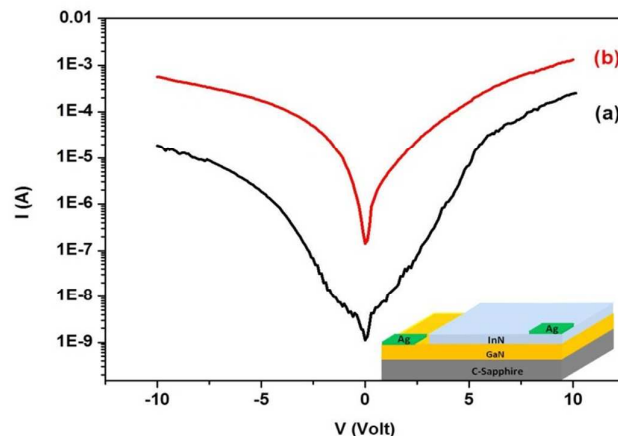


Figure 5: Room temperature I-V characteristics of InN/GaN heterojunction at room temperature a) High InN b) Low InN. Inset shows the schematics of the device structure.

Conclusions

In summary, a novel reactive ion sputtering technique has been adopted to form InN on GaN template at low temperature (300 °C) using 300 eV LENI and the valence band offset (VBO) of the grown InN/GaN heterostructure has been analyzed. The AFM analysis confirmed step like structure with large terraces ($>1 \mu\text{m}$ width) having step height $\sim 2\text{-}3 \text{ \AA}$. XPS analysis revealed the In-polarity of the sample and the presence of SEA (due to the In content at the interface) is explained. The VBO for highly nitride sample is calculated to be $0.72 \pm 0.28 \text{ eV}$ showing a straddled type InN/GaN hetero-interface band arrangement. There is plausible evidence to show the strong Fermi level pinning effect ($1.3 \pm 0.1 \text{ eV}$) above the conduction band of InN due to the upshot of metallic In at the interface. The rectifying behaviour of I-V characteristic measurement suggests that the junction between InN and GaN exhibits Schottky type behaviour. The room temperature barrier height and ideality factor obtained by using TE model were 0.72 eV and 20.8 respectively. The InN/GaN heterostructure grown at low temperature using low energy nitrogen ions with high band bending could potentially be utilized as a gate dielectric material for high electron mobility transistors where the junction between InN/GaN exhibit strong rectifying behaviour. The exact mechanism behind the SEA phenomena is still to be found, the possibility to tune surface charge density has significant implications for the design and realization of electronic and optoelectronic devices using InN.

Acknowledgement

The authors gratefully acknowledge Prof. R. C. Budhani Director, CSIR-NPL, New Delhi for their constant encouragement and support. This work is supported by Light SOLAR activity of Inorganic Solid State Lighting under CSIR-TAPSUN project NWP-55. The authors would like to thank Dr. Ritu Srivastava, Mr. Neeraj Chaudhary, Dr. N. Vijayan and Mrs. Geetanjali for AFM, GI-XRD and SIMS measurements respectively.

Reference

- 1 J. Wu, W. Walukiewicz, K. M. Yu, W. Shan, J. W. Ager, E. E. Haller, H. Lu, W. J. Schaff, W. K. Metzger, and S. Kurtz, *J. Appl. Phys.* **94**, 6477 (2003).
- 2 A. G. Bhuiyan, A. Hashimoto, and A. Yamamoto, *J. Appl. Phys.* **94**, 2779 (2003).
- 3 H. W. Seo, L. W. Tu, Q. Y. Chen, C. Y. Ho, Y. T. Lin, K. L. Wu, D. J. Jang, D. P. Norman, and N. J. Ho, *Appl. Phys. Lett.* **96**, 101114 (2010).
- 4 C. Thomidis, A. Y. Nikiforov, T. Xu, and T. D. Moustakas, *Phys. Status Solidi. C* **5**, 2301 (2008).
- 5 C. J. Neufeld, N. G. Toledo, S. C. Cruz, M. Iza, S. P. DenBaars, and U. K. Mishra, *Appl. Phys. Lett.* **93**, 143502 (2008).
- 6 S. Zhao, B. H. Le, D. P. Liu, X. D. Liu, M. G. Kibria, T. Szkopek, H. Guo, and Z. Mi, *Nano Letter* **13**, 5509 (2013).
- 7 N. Nepal, N. A. Mahadik, L. O. Nyakiti, S. B. Qadri, M. J. Mehl, J. K. Hite, and C. R Eddy Jr, *Cry. Growth and Design* **13**, 1485 (2013).
- 8 N. H. Tran, B. H. Le, S. Fan, S. Zhao, Z. Mi, B. A. Schmidt, M. Savard, G. Gervais, and K. S. A. Butcher, *Appl. Phys. Lett.* **103**, 262101 (2013).
- 9 N. Ma, X. Q. Wang, S. T. Liu, G. Chen, J. H. Pan, L. Feng, F. J. Xu, N. Tang, and B. Shen, *Appl. Phys. Lett.* **98**, 192114 (2011).
- 10 C. S. Gallinat, G. Koblmüller, J. S. Brown, S. Bernardis, J. S. Speck, G. D. Chern, E. D. Readinger, H. Shen, and Michael Wraback, *Appl. Phys. Lett.* **89**, 032109 (2006).
- 11 Q. Guo, O. Kato, and A. Yoshida, *J. Appl. Phys.* **73**, 7969 (1993).
- 12 M. T. Currie, C. W. Leitz, T. A. Langdo, G. Taraschi, and E. A. Fitzgerald, *J. Vac. Sci. Technol. B-Microelectronics and Nanometer Structures.* **19**, 2228 (2001).
- 13 G. Martin, A. Botchkarev, A. Rockett, and H. Morkoç, *Appl. Phys. Lett.* **68**, 2541 (1996).
- 14 Z. Li, B. Zhang, J. Wang, J. Liu, X. Liu, S. Yang, Q. Zhu, and Z. Wang, *Nanoscale Res. Lett.* **6**, 193 (2011).
- 15 P. D. C. King, T. D. Veal, S. A. Hatfield, P. H. Jefferson, C. F. McConville, C. E. Kendrick, C. H. Swartz, and S. M. Durbin, *Appl. Phys. Lett.* **91**, 112103 (2007).
- 16 J. Wu, W. Walukiewicz, W. Shan, K. M. Yu, J. W. Ager, S. X. Li, E. E. Haller, H. Lu, and W. J. Schaff, *J. Appl. Phys.* **94**, 4457 (2003).
- 17 X. Wang, S. Liu, N. Ma, L. Feng, G. Chen, F. Xu, N. Tang, S. Huang, K. J. Chen, S. Zhou, and B. Shen, *Appl. Phys. Express* **5**, 015502 (2012).
- 18 B. Roul, M. K. Rajpalke, T. N. Bhat, M. Kumar, N. Sinha, A. T. Kalghatgi, and S. B. Krupanidhi, *J. Appl. Phys.* **109**, 044502 (2011).
- 19 A. R. Arehart, B. Moran, J. S. Speck, U. K. Mishra, S. P. DenBaars, and S. A. Ringel, *J. Appl. Phys.* **100**, 023709 (2006).
- 20 K. Cinar, N. Yildirim, C. Coskun, and A. Turut, *J. Appl. Phys.* **106**, 073717 (2009).
- 21 Y. J. Lin, *J. Appl. Phys.* **106**, 013702 (2009).
- 22 K. Wang, C. Lian, N. Su, D. Jena, and J. Timler, *Appl. Phys. Lett.* **91**, 232117 (2007).
- 23 C. F. Shih, N. C. Chen, and C. Y. Tseng, *Thin Solid Films.* **516**, 5016 (2008).
- 24 H. P. Maruska and J. J. Tietjen, *Appl. Phys. Lett.* **15**, 327 (1969).
- 25 P. D. C. King, T. D. Veal, P. H. Jefferson, and C. F. McConville, T. Wang, P. J. Parbrook, H. Lu, and W. J. Schaff, *Appl. Phys. Lett.* **90**, 132105 (2007).
- 26 I. Mahboob, T. D. Veal, C. F. McConville, H. Lu, and W. J. Schaff, *Phys. Rev. Lett.* **92**, 036804 (2004).
- 27 H. Lu, W. J. Schaff, L. F. Eastman, and C. E. Stutz, *Appl. Phys. Lett.* **82**, 1736 (2003).
- 28 I. Mahboob, T. D. Veal, L. F. J. Piper, and C. F. McConville, *Phys. Rev. B* **69**, 201307 (2004).
- 29 S. X. Li, K. M. Yu, J. Wu, R. E. Jones, W. Walukiewicz, J. W. Ager III, W. Shan, E. E. Haller, H. Lu, and W. J. Schaff, *Phys. Rev. B* **71**, 161201(R) (2005).
- 30 P. D. C. King, T. D. Veal, C. F. McConville, J. Zuniga-Perez, V. Munoz-Sanjose, M. Hopkinson, E. D. L. Rienks, M. Fuglsang Jensen, and Ph. Hofmann *Phys. Rev. Lett.* **104**, 256803 (2010).
- 31 D. Segev and C. G. V. D. Walle, *Europhys. Lett.* **76**, 305 (2006).
- 32 L. F. J. Piper, T. D. Veal, M. J. Lowe, and C. F. McConville, *Phys. Rev. B* **73**, 195321 (2006).
- 33 J. L. Rouviere, J. L. Weyher, M. Seelmann-Eggebert, and S. Porowski *Appl. Phys. Lett.* **73**, 668 (1998).
- 34 Y. Enta, S. Suzuki, S. Kono, and T. Sakamoto, *Phys. Rev. B* **39**, 5524 (1989).
- 35 T. Kawabata, F. Okuyama, and M. Tanemura, *J. Appl. Phys.* **69**, 3723 (1991).
- 36 J. A. Taylor, G. M. Lancaster, A. Ignatiev, and J. W. Rabalais, *J. Chem. Phys.* **68**, 1776 (1978).
- 37 B. Heying, E. J. Tarsa, C. R. Elsass, P. Fini, S. P. DenBaars, and J. S. Speck *J. Appl. Phys.* **85**, 6470 (1999).
- 38 H. Kim, Z. L. Guan, Q. Sun, A. Kahn, J. Han, and A. Nurmikko, *Appl. Phys. Lett.* **107**, 113707 (2010).
- 39 M. Tangi, J. Kuyyalil, and S. M. Shivaprasad, *J. Appl. Phys.* **114**, 153501 (2013).
- 40 A. R. Smith, R. M. Feenstra, D. W. Greve, M. S. Shin, M. Skowronski, J. Neugebauer, and J. E. Northrup, *J. Vac. Sci. Technol. B* **16**, 2242 (1998).
- 41 J. E. Northrup, J. Neugebauer, R. M. Feenstra, and A. R. Smith, *Phys. Rev. B* **61**, 9932 (2000).
- 42 J. Wu, *J. Appl. Phys.* **106**, 011101 (2009).
- 43 X. Wang, S. B. Che, Y. Ishitani, and A. Yoshikawa, *J. Appl. Phys.* **99**, 073512 (2006).
- 44 E. Dimakis, E. Iliopoulos, K. Tsagaraki, and A. Georgakilas, *Appl. Phys. Lett.* **86**, 133104 (2005).
- 45 R. S. Q. Fareed, R. Jain, R. Gaska, M. S. Shur, J. Wu, W. Walukiewicz, and M. S. Khan, *Appl. Phys. Lett.* **84**, 1892 (2004).
- 46 S. A. Chamber, T. Droubay, T. C. Kaspar, and M. Gutowski, *J. Vac. Sci. Technol. B* **22**, 2205 (2004).
- 47 H. W. Jang, K. W. Ihm, T. H. Kang, J. H. Lee, and J. L. Lee, *Phys. Stat. Sol. (b)* **240**, 451 (2003).
- 48 Q. X. Guo, M. Nishio, H. Ogawa, A. Wakahara, and A. Yoshida, *Phys. Rev. B* **58**, 15304 (1998).
- 49 L. Ley, R. A. Pollak, F. R. McFeely, S. P. Kowalczyk, and D. A. Shirley, *Phys. Rev. B* **9**, 600 (1974).
- 50 P. D. C. King, T. D. Veal, P. H. Jefferson, S. A. Hatfield, L. F. J. Piper, C. F. McConville, F. Fuchs, J. Furthmüller, F. Bechstedt, H. Lu, and W. J. Schaff, *Phys. Rev. B* **77**, 045316 (2008).
- 51 T. D. Veal, P. D. C. King, P. H. Jefferson, L. F. J. Piper, C. F. McConville, H. Lu, W. J. Schaff, P. A. Anderson, S. M. Durbin, D. Mute, H. Naoi, and Y. Nanishi, *Phys. Rev. B* **76**, 075313 (2007).
- 52 P. D. C. King, T. D. Veal, C. F. McConville, F. Fuchs, J. Furthmüller, F. Bechstedt, P. Schley, R. Goldhahn, J. Schörmann, D. J. As, K. Lischka, D. Muto, H. Naoi, Y. Nanishi, H. Lu, and W. J. Schaff, *Appl. Phys. Lett.* **91**, 092101 (2007).

- 53 L. F. J. Piper, T. D. Veal, P. H. Jefferson, C. F. McConville, F. Fuchus, J. Furtmuller, F. Bechstedt, H. Lu, and W. J. Schaff, *Phys. Rev B* **72**, 245319 (2005).
- 54 C. G. Van de Walle, and J. Neugebauer, *Nature* **423**, 626 (2003).
- 55 P. D. C. King, T. D. Veal, C. E. Kendrick, L. R. Bailey, S. M. Durbin, and C. F. McConville, *Phys. Rev. B* **78**, 033308 (2008).
- 56 K. Wang, C. Lian, N. Su, D. Jena, and J. Timler, *Appl. Phys. Lett.* **91**, 232117 (2007).
- 57 C.-T. Kuo, S. C. Lin, K.-K. Chang, H.-W. Shiu, L.-Y. Chang, C.-H. Chen, S.-J. Tang, and S. Gwo, *Appl. Phys. Lett.* **98**, 052101 (2011).
- 58 A. Eisenhardt, S. Krischok, and M. Himmerlich, *Appl. Phys. Lett.* **102**, 231602 (2013).
- 59 N. C. Chen, P. H. Chang, Y. N. Wang, H. C. Peng, W. C. Lien, C. F. Shih, Chin-An Chang, and G. M. Wu, *Appl. Phys. Lett.* **87**, 212111 (2005).
- 60 R. P. Bhatta, B. D. Thoms, A. Weerasekera, A. G. U. Perera, M. Alevli, and N. Dietz, *J. Vac. Sci. Technol. A* **25**, 967 (2007).
- 61 L. Wang, M. I. Nathan, T. Lim, M. A. Khan, and Q. Chen, *Appl. Phys. Lett.* **68**, 1267 (1996).
- 62 X. M. Shen, D. G. Zhao, Z. S. Liu, Z. F. Hu, H. Yang, and J. W. Liang, *Solid-State Electron.* **49**, 847 (2005)

